ORIGINAL ARTICLE

Journal Section

Optimal Observer-based Output Feedback Controller for Traffic Congestion with Bottleneck

Lina Guan[1,2,3,*] | **Liguo Zhang**[1,2] | **Christophe Prieur**[3]

[1]Faculty of Information Technology, Beijing University of Technology, Beijing, China

[2]Key Laboratory of Computational Intelligence and Intelligent Systems, 100124, Beijing, China

[3]Univ. Grenoble Alpes, CNRS, Grenoble INP, GIPSA-lab, 38000 Grenoble, France

[*]Corresponding author

Correspondence
Gipsa-lab, Grenoble Campus 11 rue des Mathématiques, BP 46, 38402 Saint Martin d'Hères Cedex, France
Email: lina.guan@grenoble-inp.fr

Funding information
This work is supported by the National Natural Science Foundation of China (NSFC, Grant No. 61873007), the Beijing Natural Science Foundation (Grant No. 1182001), and a research grant from project PHC CAI YUANPEI under grant number 44029QD, and by MIAI @ Grenoble Alpes (ANR-19-P3IA-0003).

This paper designs an optimal observer-based output feedback control for traffic breakdown to dissolve traffic congestion using the backstepping method and optimization. The linearized Aw-Rascle-Zhang model is used to represent the congested traffic dynamics resulting from traffic breakdown. Based on the factors leading to traffic breakdown, we take into account the boundary conditions consisting of a boundary with a constant density and a speed drop at the upstream inlet of a bottleneck, and a boundary with a disturbance of inflow (high traffic demand) at the inlet of the road segment under consideration. To dissolute traffic congestion, a dynamic feedback controller is designed at the upstream boundary. By using the backstepping approach, an observer-based output feedback controller is computed to guarantee the integral input-to-state stability of the closed-loop system. By establishing an optimization problem and solving it, the optimal value of the considered class controller is obtained. The performance of the output feedback controller is also validated by numerical simulations.

KEYWORDS
Linearized ARZ traffic flow model, High traffic demand, Backstepping, Observer-based output feedback control, Optimization

Abbreviations: ARZ, Aw-Rascle-Zhang; PDEs, partial differential equations; iISS, integral input-to-state stability.

1 | INTRODUCTION

Traffic congestion resulting from traffic breakdown is an ubiquitous problem resulting in the increase of fuel consumption and unsafe driving conditions. In the real world, traffic breakdown usually arises from the combination of three factors: high traffic demand, bottlenecks, and disturbances caused by individual drivers (see [1]). High traffic demand is the inflow indicating the potential average traffic flow on the main road and exceeding the bottleneck capacity, such as during rush hours. The most bottlenecks include flow-conserving bottlenecks and non-flow-conserving bottlenecks with additional sources and sinks, for example, on-ramp and off-ramp bottlenecks, or permanent and temporary types such as the blocking effect resulted from the accidents or traffic lights. Local disturbances are caused by individual drivers, such as abrupt lane changes, braking maneuvers, or other un-anticipated actions. The disturbances often lead to a platoon of vehicles following each other at small time gaps which eventually becomes the first propagating upstream traffic wave of a triggered stop-and go state.

There are several macroscopic models of traffic dynamics including first order Lighthill-Whitham-Richards (LWR) model (see [2] and [3]), second order Payne-Whitham (PW) model (see [4] and [5]) and second order Aw-Rascle-Zhang (ARZ) model (see [6] and [7]). The first-order LWR model represents density-velocity relation in equilibrium and fails to model stop-and-go traffic. PW model consists of momentum equation and conservation law, and it is a nonlinear second-order partial differential equations (PDEs) that describe deviations from density-velocity equilibrium. It is shown that disturbances in PW model travel faster than traffic velocity in [8] and [9]. Consequently, vehicles on freeway are effected by both behind and front. [7] showed that drivers mostly respond to the traffic in front of them. [6] and [7] separately brought forward a new velocity equation to solve this problem. Afterwards, ARZ model is derived from the combination of these two models through suitable definition and coefficients. Two-dimensional traffic dynamic model for large scale traffic networks is introduced in [10].

In order to stabilize hyperbolic systems of the highway traffic, it is natural to use boundary feedback control on available control signals as ramp metering or variable speed limits on a road. In order to design a boundary control law for the linearized ARZ traffic flow model, spectral analysis is applied in [11]. Paper [12] proves the local stability of a positive hyperbolic system and [13] designs a proportional-integral (PI) boundary feedback controller to stabilize the oscillations of the traffic parameters on a freeway by Lyapunov method. [14] presents explicit boundary conditions which guarantee the Lyapunov stability of the weak entropy solution to the scalar conservation law with convex flux.

In this paper, we use backstepping method to derive a boundary feedback controller to dissolve traffic congestion resulting from traffic breakdown. The backstepping approach is the extension of Volterra integral transformations and can be used to systematically design controller and observers for linear PDEs. For the infinite-dimensional system, the controllers and observers can be derived directly and all analysis can be done without discretization before implementing on a computer. The rationale behind the backstepping method is the following: through constructing an appropriate Volterra integral transformation, the original PDE system is mapped to an integral input-to-state stable (iISS) target system. The original system inherits the stability property thanks to the invertibility of backstepping transformation. The kernels derived from the backstepping transformation are adopted as gains of the original system feedback controller.

The backstepping method for hyperbolic PDEs was initially introduced by [15], [16] and [17]. For backstepping boundary control design of 2×2 coupled hyperbolic systems, there are some theoretical results obtained recently. [18] uses a backstepping transformation to design a full-state feedback control law and derives H^2 exponential stability for a quasilinear 2×2 system of first-order hyperbolic PDEs. Robust output regulation problem for boundary controlled linear 2×2 hyperbolic systems is solved in [19]. By implementing the finite-time state feedback regulator with disturbance observers, the finite-time output regulation problem is solved in [20]. Two closely related state feedback

adaptive control laws are designed for stabilization of linear hyperbolic system with constant but uncertain in-domain and boundary parameters in [21]. In [22], a boundary observer for nonlinear ARZ traffic flow model is designed to estimate the information of traffic states using the backstepping method. An output feedback controller is designed for the underactuated cascade network of interconnected PDEs systems using backstepping in [23].

In consideration of the limits of technology and cost, there have been works inspired by [24], designing an observer-based output feedback control law for the linearized ARZ traffic flow model by using backstepping transformations (see also [25]). Although [26] has used the same method to deal with the disturbance rejection problem from the oil and gas industry, this paper in the first work to design an optimal observer-based output boundary control of traffic breakdown to remove or weaken the effect of high traffic demand acting as a given time-varying disturbance input with the fastest convergence rate. Moreover, we design a controller and an observer respectively with a time-depending integral term to reject disturbances by using backstepping transformation mapping the error system into an iISS target system with a time-varying disturbance term. We use Lyapunov approach to prove the iISS of this target system whose boundary control strategy is PI boundary control. Inspired by [27], we can compute the kernels of backstepping transformations using a general expression of the kernel functions.

In order to solve the traffic bottleneck problem, the extremum seeking control with delay compensation is used in [28] to obtain the optimal density that maximizes the outflow and mitigates the traffic congestion on the considered roadway. Additionally, another difference is that the traffic flow dynamics is described by the LWR macroscopic partial differential equation model. On the basis of the Kerner–Klenov–Wolf (KKW) model of three-phase traffic flow theory, the traffic flow model of expressway ramp system under the accident conditions is proposed in [29], and the combined bottleneck effect of accidents on the traffic flow under the open boundary condition is simulated and analyzed. Considering the LWR model with bounded acceleration, the optimal location problem is analytically identified, formulated, and solved for variable speed limit application areas inside a lane drop bottleneck in [30].

This paper is organized as follows. In Section 2, the linearized ARZ traffic flow model with boundary disturbances for congested traffic deriving from traffic breakdown is derived by making use of coordinate transformation and linearization around the steady state. Using backstepping transformation to map the linearized ARZ traffic flow model into an iISS target system, we obtain a full state feedback controller in Section 3. An observer-based output feedback controller is designed in Section 4. In Section 5, the optimization problem is discussed and the results of numerical simulations are provided. The paper ends with concluding remarks in Section 6.

2 | TRAFFIC FLOW SYSTEM AND CONTROL PROBLEM

2.1 | ARZ traffic flow system and problem statement

The Aw-Rascle-Zhang model is a typically local second-order macroscopic traffic flow model composed of the following continuity and acceleration equations:

$$\rho_t + (v\rho)_x = 0, \tag{1}$$

$$v_t + \left(v - \rho p'(\rho)\right) v_x = \frac{V_e(\rho) - v}{\tau}, \tag{2}$$

with an independent space variable x in $(0, L)$ on a road section of length L, and an independent time variable t in $[0, \infty)$. As the locally aggregated quantities, the traffic density $\rho(x, t)$ is defined as the number of vehicles per unit length at time t, the mean speed $v(x, t)$ is the average speed of the vehicles passing the location x for a fixed time interval. The speed adaptation time τ is a constant and corresponds to the inverse of the agility. In the previous model,

the steady-state speed $V_e(\rho)$ is the speed-density relation given by Greenshields model in [31] as

$$V_e(\rho) = v_f \left(1 - \frac{\rho}{\rho_m}\right), \tag{3}$$

where v_f is the free flow speed, ρ_m is the maximum density. The speed adaptation term or relaxation term located in the right side of equation (2) describes the mean acceleration of the vehicles in the local neighborhood for reaching the steady-state speed.

The traffic pressure $p(\rho)$ is an increasing function of density defined as

$$p(\rho) = v_f - V_e(\rho) = \frac{v_f}{\rho_m}\rho. \tag{4}$$

Let $\omega = v + \frac{v_f}{\rho_m}\rho$, then (1) and (2) are written as

$$\omega_t + v\omega_x = \frac{v_f - \omega}{\tau}, \tag{5}$$

$$v_t + (2v - \omega)v_x = \frac{v_f - \omega}{\tau}. \tag{6}$$

In (6), the propagation velocity $2v - \omega > 0$ stands for the weak interactions between the vehicles, the traffic wave propagates with the traffic flow (downstream) at this characteristic velocity in free traffic. Usually, the propagation velocity of the traffic wave is slightly less than the average free-flow vehicle speed in free traffic. Reversely, the characteristic velocity $2v - \omega < 0$ represents the traffic waves moves against the traffic flow (upstream) in congested traffic due to the reaction of the drivers to their respective leading vehicles. In this paper, we take into account the control problem of perturbation in congested traffic situations.

Denote by $(\omega^*, v^*)^\top$ in $C^1([0, L]; \mathbb{R}^2)$ a steady state of the system (5)-(6) such that $2v^*(x) - \omega^*(x) < 0$ for all $x \in [0, L]$ on a stable and inhomogeneous road (with speed and density gradients). Note that it depends on the space variable x and the corresponding density is $\rho^*(x) = \frac{\rho_m}{v_f}(\omega^*(x) - v^*(x))$. The deviations from the system states $(\omega, v)^\top$ are defined as

$$\widetilde{\omega}(x, t) = \omega(x, t) - \omega^*(x), \tag{7}$$

$$\widetilde{v}(x, t) = v(x, t) - v^*(x), \tag{8}$$

then the quasilinear deviation system is obtained,

$$\widetilde{\omega}_t(x, t) + \Lambda_1(\widetilde{\omega}, \widetilde{v}, x)\widetilde{\omega}_x(x, t) + \widetilde{v}(x, t)\frac{\mathrm{d}\omega^*(x)}{\mathrm{d}x} + \frac{\widetilde{\omega}(x, t)}{\tau} = 0, \tag{9}$$

$$\widetilde{v}_t(x, t) + \Lambda_2(\widetilde{\omega}, \widetilde{v}, x)\widetilde{v}_x(x, t) + (2\widetilde{v}(x, t) - \widetilde{\omega}(x, t))\frac{\mathrm{d}v^*(x)}{\mathrm{d}x} + \frac{\widetilde{\omega}(x, t)}{\tau} = 0, \tag{10}$$

with two characteristic velocities

$$\Lambda_1(\widetilde{\omega}, \widetilde{v}, x) = \widetilde{v}(x, t) + v^*(x), \tag{11}$$

$$\Lambda_2(\widetilde{\omega}, \widetilde{v}, x) = 2\widetilde{v}(x, t) - \widetilde{\omega}(x, t) + 2v^*(x) - \omega^*(x), \tag{12}$$

where $\Lambda_1(\widetilde{\omega}, \widetilde{v}, x) > 0$, $\Lambda_2(\widetilde{\omega}, \widetilde{v}, x) < 0$.

As described in [1], beyond the deterministic factors causing the traffic breakdown, high traffic demand is the most effective ingredient. The disturbances caused by bottlenecks or individual drivers can not grow and propagate on account of unconditional stability, if the traffic load is low enough. However, in spite of the absolute stability, traffic breakdown will take place with inflow in excess of the capacity of bottlenecks on the considered road segment. The local capacity reduction is the decisive attribute of characterizing the obstructing effect of a bottleneck. Furthermore, we can not predict the time and location of individual traffic breakdown due to the stochastic and single-vehicle natures of disturbances caused by individual drivers.

In order to increase the efficiency and stability of traffic flow, we solve the control problem (in an optimal way that is introduced late precisely) of high traffic demand by ramp metering in the presence of a bottleneck and disturbances on the road. Considering a road segment with a constant density ρ^*_{out} and a speed drop $v_-(L,t) > v_+(L,t)$ at the boundary of the bottleneck, the diagram of the control model is illustrated in Figure 1. The control is defined as $U(t)$ and would depend only on t.

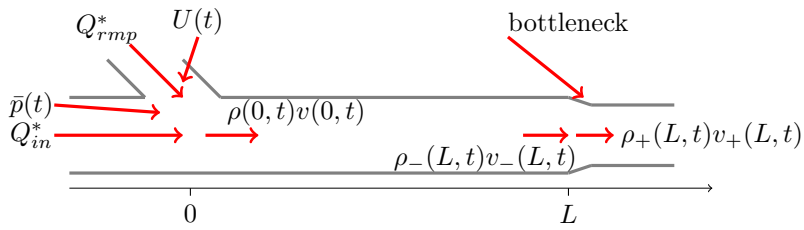

FIGURE 1 The traffic flow on a road segment with an downstream on-ramp bottleneck.

To be more specific, the boundary condition at $x = L$ is, for all $t \geq 0$,

$$\rho_-(L,t) = \rho_+(L,t) = \rho^*_{out}. \tag{13}$$

On the basis of the conservation of vehicle flows, the boundary condition with disturbances caused by high traffic demand at the upstream inlet $x = 0$ can be derived,

$$Q^*_{in} + Q^*_{rmp} + U(t) + \bar{p}(t) = \rho(0,t)v(0,t), \tag{14}$$

where $Q^*_{rmp} > 0$ denotes the steady-state on-ramp flow at the segment boundary upstream, Q^*_{in} denotes the steady-state inflow at the upstream boundary, and they satisfy $Q^*_{in} + Q^*_{rmp} = \rho^*(0)v^*(0)$; $\bar{p}(t)$ is the unknown disturbances of inflow serving as exogenous variable (externally given model input) depending on time t, the difference between the measured speed at the inlet $v(0,t)$ and the corresponding steady state $v^*(0) \geq 0$ acts as the model output, i.e.,

$$y(t) = v(0,t) - v^*(0), \tag{15}$$

and the control law $U(t)$ is implemented by the on-ramp metering at upstream boundary of the main road. Ramp metering temporarily reduces the traffic throughput and delays to increase it to prevent a traffic breakdown and the associated capacity drop. We compute the optimal gains of controller $U(t)$ depending on the output $y(t)$ only, so that the system states converge to the steady state at the fastest speed, up to a constant depending on the size of the

disturbance $\bar{p}$.

2.2 | Coordinate transformation and linearization around steady state

In this section, in order to solve the previous problem, we perform a change of variables and we linearize the model. Define the coordinate transformation

$$\epsilon_1(x,t) = \psi_1(x)\widetilde{\omega}(x,t), \tag{16}$$

$$\epsilon_2(x,t) = \psi_2(x)\widetilde{v}(x,t), \tag{17}$$

with

$$\psi_1(x) = \exp\left(\int_0^x \frac{1}{\tau v^*(s)}\,\mathrm{d}s\right), \tag{18}$$

$$\psi_2(x) = \exp\left(\int_0^x \frac{\mathrm{d}v^*(s)}{\mathrm{d}s}\cdot\frac{2}{2v^*(s)-\omega^*(s)}\,\mathrm{d}s\right), \tag{19}$$

for all x in $(0, L)$, then the system (9)-(10) is rewritten as follows,

$$\epsilon_{1t} + \Lambda_1(\epsilon_1,\epsilon_2,x)\epsilon_{1x} + c_1(x)\epsilon_2 - \frac{\psi_2^{-1}(x)}{\tau v^*(x)}\epsilon_1\epsilon_2 = 0, \tag{20}$$

$$\epsilon_{2t} + \Lambda_2(\epsilon_1,\epsilon_2,x)\epsilon_{2x} + c_2(x)\epsilon_1 + \frac{\mathrm{d}v^*(x)}{\mathrm{d}x}\cdot\frac{2\epsilon_2}{2v^*(x)-\omega^*(x)}\left(2\psi_2^{-1}(x)\epsilon_2 - \psi_1^{-1}(x)\epsilon_1\right) = 0, \tag{21}$$

with

$$\Lambda_1(\epsilon_1,\epsilon_2,x) = \psi_2^{-1}(x)\epsilon_2 + v^*(x), \tag{22}$$

$$\Lambda_2(\epsilon_1,\epsilon_2,x) = 2\psi_2^{-1}(x)\epsilon_2 - \psi_1^{-1}(x)\epsilon_1 + 2v^*(x) - \omega^*(x), \tag{23}$$

$$c_1(x) = \frac{\mathrm{d}\omega^*(x)}{\mathrm{d}x}\psi_1(x)\psi_2^{-1}(x), \tag{24}$$

$$c_2(x) = \left(\frac{1}{\tau} - \frac{\mathrm{d}v^*(x)}{\mathrm{d}x}\right)\psi_1^{-1}(x)\psi_2(x). \tag{25}$$

From the linearization of the quasilinear equation (20)-(21), we can derive

$$\epsilon_{1t}(x,t) + \lambda_1(x)\epsilon_{1x}(x,t) + c_1(x)\epsilon_2(x,t) = 0, \tag{26}$$

$$\epsilon_{2t}(x,t) - \lambda_2(x)\epsilon_{2x}(x,t) + c_2(x)\epsilon_1(x,t) = 0, \tag{27}$$

with

$$\lambda_1(x) = v^*(x) > 0, \tag{28}$$

$$\lambda_2(x) = \omega^*(x) - 2v^*(x) > 0. \tag{29}$$

Therefore, from (13) and the transformations (7)-(8) and (16)-(17), the boundary condition at $x = L$ may be

achieved as, for all $t \geq 0$,

$$\epsilon_2(L,t) = \frac{1}{\kappa}\epsilon_1(L,t), \tag{30}$$

with

$$\kappa = \psi_1(L)\psi_2^{-1}(L). \tag{31}$$

The following linearized boundary condition at $x = 0$ is derived from (14),

$$\epsilon_1(0,t) = q_1\epsilon_2(0,t) + q_2\left(U(t) + \bar{p}(t)\right), \tag{32}$$

with

$$q_1 = \frac{2v^*(0) - \omega^*(0)}{v^*(0)}, \tag{33}$$

and

$$q_2 = \frac{v_f}{\rho_m v^*(0)}. \tag{34}$$

We reformulate the previous control problem as follows. We seek the optimal parameters of an observer-based output feedback control law at the upstream of considerated road section in order to remove or weaken the effect of high traffic demand and stabilize the linearized ARZ traffic flow model. Inspired by [24], [18], but using different backstepping transformations due to different boundary conditions, we can design a new observer-based output feedback control law. Firstly, we derive a full-state feedback control law with kernels from the backstepping transformation mapping the original system to an iISS target system. An observer is designed to estimate the states of the linearized ARZ traffic flow system. The precise estimation to the states of the original system is guaranteed by the analytic expressions of injection gains which are obtained by the backstepping transformation mapping the error system (derived by subtracting the state-estimate system from the original system) to the same target system. Finally, the optimal parameters of the observer-based output feedback controller are derived by solving the optimization problem with the objective function, defined as the highest rate of exponential convergence.

3 | FULL-STATE FEEDBACK CONTROLLER

The main results of this section are the proof of the iISS of a target system with PI boundary conditions and obtaining a full-state feedback controller through backstepping transformation.

3.1 | Target system

Firstly, we introduce a target system,

$$\alpha_t(x,t)+\lambda_1(x)\alpha_x(x,t)=0, \tag{35}$$

$$\beta_t(x,t)-\lambda_2(x)\beta_x(x,t)=0, \tag{36}$$

$$\alpha(0,t)=q_1\beta(0,t)+k_i\eta(t), \tag{37}$$

$$\beta(L,t)=\frac{1}{\kappa}\alpha(L,t), \tag{38}$$

where $k_i \in \mathbb{R}\setminus\{0\}$ is an integral tuning parameter, and

$$\eta(t)=\int_0^t(\beta(0,s)-\alpha(0,s))\,\mathrm{d}s+k_i^{-1}q_2\bar{p}(t). \tag{39}$$

According to the following theorem, the target system (35)-(39) is integral input-to-state stable for L^2-norm. The symbol $*$ stands for a symmetric block in the following content.

Theorem 1 (Integral Input-to-state Stability of Target System) *Assume there exist positive constants μ, θ, p_1, p_2, p_4, q_3, q_4 and constant p_3 such that for all x in $[0,L]$,*

$$M_1=\begin{bmatrix} M_1^{11} & M_1^{12} & M_1^{13}\\ * & M_1^{22} & M_1^{23}\\ * & * & M_1^{33}\end{bmatrix}\geq 0 \tag{40}$$

with

$$M_1^{11}=p_1e^{-\mu L}-\frac{p_2}{\kappa^2}e^{\mu L}, \tag{41}$$

$$M_1^{12}=0, \tag{42}$$

$$M_1^{13}=-\frac{p_3}{2\kappa}e^{\frac{\mu}{2}L}, \tag{43}$$

$$M_1^{22}=-p_1q_1^2+p_2-\frac{3q_4L}{2}|p_3|(1-q_1)^2, \tag{44}$$

$$M_1^{23}=-p_1q_1k_i+\frac{p_3}{2}-\frac{1}{2}p_4L(1-q_1), \tag{45}$$

$$M_1^{33}=-p_1k_i^2-\frac{3q_4L}{2}|p_3|k_i^2+(1-m)L(p_4k_i-\frac{q_3}{2}|k_i^{-1}|q_2p_4), \tag{46}$$

$$\begin{bmatrix}\frac{p_2}{\lambda_2(x)} & \frac{p_3}{2\lambda_2(x)}\\ \frac{p_3}{2\lambda_2(x)} & \frac{p_4}{2}\end{bmatrix}>0, \tag{47}$$

$$m(k_i-\frac{q_3}{2}|k_i^{-1}|q_2)>\frac{\theta}{2}, \tag{48}$$

$$\mu>\frac{\theta}{\lambda_1(x)}, \tag{49}$$

and

$$\begin{bmatrix} \mu p_2 - \frac{|p_3|}{2q_4\lambda_2^2(x)} - \frac{\theta p_2}{\lambda_2(x)} & \frac{\mu p_3}{4} - \frac{\theta p_3}{2\lambda_2(x)} \\ \frac{\mu p_3}{4} - \frac{\theta p_3}{2\lambda_2(x)} & m(p_4 k_i - \frac{q_3}{2}|k_i^{-1}|q_2 p_4) - \frac{\theta p_4}{2} \end{bmatrix} > 0. \tag{50}$$

Then there exists positive constants Ω_1, b_1 such that, for any $z_0 = (\alpha(\cdot,0), \beta(\cdot,0), \eta(0))^\top$ in $L^2((0,L);\mathbb{R}^3)$, and for any $\bar{p}$ such that $\dot{\bar{p}} \in \mathcal{L}^2[0,\infty)$, the solution $z = (\alpha, \beta, \eta)^\top$ to the system (35)-(39) satisfies, for all $t \geq 0$,

$$\|z(\cdot,t)\|^2_{L^2((0,L);\mathbb{R}^3)} \leq \Omega_1 e^{-\theta t}\|z_0\|^2_{L^2((0,L);\mathbb{R}^3)} + b_1 \int_0^t \dot{\bar{p}}^2(s)\,\mathrm{d}s. \tag{51}$$

Remark Some observations follow

- From the inequality condition (48) in Theorem 1, it follows that the parameters m and k_i have the identical sign, i.e., $mk_i > 0$.
- Note that the first term at the right-hand side of inequality (51) is continuous, decreasing with respect to t and converges to zero as t goes to infinity. Since $b_1 > 0$, the second term is increasing and tends to the $\mathcal{L}^2$ norm of $\dot{\bar{p}}$. That is, the integral input-to-state stability of system (35)-(39) holds, by following the terminology of [32] and [33].

Proof The following candidate Lyapunov function is proposed for the purpose of analyzing the stability of the system (35)-(39),

$$V = \int_0^L \begin{bmatrix} \alpha(x,\cdot) \\ \beta(x,\cdot) \\ \eta(\cdot) \end{bmatrix}^\top P(x) \begin{bmatrix} \alpha(x,\cdot) \\ \beta(x,\cdot) \\ \eta(\cdot) \end{bmatrix} \mathrm{d}x = V_1 + V_2 + V_3 + V_4, \tag{52}$$

with

$$P(x) = \begin{bmatrix} \frac{p_1}{\lambda_1(x)} e^{-\mu x} & 0 & 0 \\ * & \frac{p_2}{\lambda_2(x)} e^{\mu x} & \frac{p_3}{2\lambda_2(x)} e^{\frac{\mu x}{2}} \\ * & * & \frac{p_4}{2} \end{bmatrix}, \quad \text{for all } x \in [0,L] \tag{53}$$

and

$$V_1 = p_1 \int_0^L \frac{e^{-\mu x}}{\lambda_1(x)} \alpha^2(x,\cdot)\,\mathrm{d}x, \tag{54}$$

$$V_2 = p_2 \int_0^L \frac{e^{\mu x}}{\lambda_2(x)} \beta^2(x,\cdot)\,\mathrm{d}x, \tag{55}$$

$$V_3 = p_3 \eta(\cdot) \int_0^L \frac{e^{\frac{\mu x}{2}}}{\lambda_2(x)} \beta(x,\cdot)\,\mathrm{d}x, \tag{56}$$

$$V_4 = \frac{p_4 L}{2} \eta^2(\cdot). \tag{57}$$

On account of inequality (47) with $p_1 > 0, \lambda_1(x) > 0$, the following inequality holds for all x in $[0, L]$,

$$\begin{bmatrix} \frac{p_1}{\lambda_1(x)} e^{-\mu x} & 0 \\ * & \left(\frac{p_2}{\lambda_2(x)} - \frac{p_3^2 p_4^{-1}}{2\lambda_2^2(x)} \right) e^{\mu x} \end{bmatrix} > 0. \tag{58}$$

Using Schur complement with $p_4 > 0$, $P(x)$ is symmetric positive definite for all x in $[0, L]$. Therefore,

$$\lambda_{\min} \cdot \left(\int_0^L \left(\alpha^2(x, \cdot) + \beta^2(x, \cdot) \right) \mathrm{d}x + L\eta^2(\cdot) \right) \leq V \leq \lambda_{\max} \cdot \left(\int_0^L \left(\alpha^2(x, \cdot) + \beta^2(x, \cdot) \right) \mathrm{d}x + L\eta^2(\cdot) \right), \tag{59}$$

where

$$\lambda_{\min} = \min_{x \in [0,L]} \lambda(P(x)), \tag{60}$$

$$\lambda_{\max} = \max_{x \in [0,L]} \lambda(P(x)). \tag{61}$$

In the previous equation, $\lambda(P(x))$ is the eigenvalue of $P(x)$ and $\lambda_{\min} > 0, \lambda_{\max} > 0$.
From (39), one can derive

$$\dot{\eta}(t) = \beta(0, t) - \alpha(0, t) + k_i^{-1} q_2 \dot{\tilde{p}}(t). \tag{62}$$

The time derivatives of (54)-(57) along the solutions to the system (35)-(39) are computed using integrations by parts

in (54)-(56), Young's inequality in (56), and (62), for all $t \geq 0$,

$$\begin{aligned}
\dot{V}_1 &= 2p_1 \int_0^L \frac{e^{-\mu x}}{\lambda_1(x)} \alpha(x,t)\alpha_t(x,t)\,\mathrm{d}x \\
&= -p_1\alpha^2(x,t)e^{-\mu x}\Big|_0^L - \mu p_1 \int_0^L \alpha^2(x,t)e^{-\mu x}\,\mathrm{d}x \\
&= p_1\left(q_1\beta(0,t) + k_i\eta(t)\right)^2 - p_1 e^{-\mu L}\alpha^2(L,t) - \mu p_1 \int_0^L \alpha^2(x,t)e^{-\mu x}\,\mathrm{d}x, \qquad (63)\\
\dot{V}_2 &= 2p_2 \int_0^L \frac{e^{\mu x}}{\lambda_2(x)} \beta(x,t)\beta_t(x,t)\,\mathrm{d}x \\
&= p_2\beta^2(x,t)e^{\mu x}\Big|_0^L - \mu p_2 \int_0^L \beta^2(x,t)e^{\mu x}\,\mathrm{d}x \\
&= \frac{p_2}{\kappa^2}e^{\mu L}\alpha^2(L,t) - p_2\beta^2(0,t) - \mu p_2 \int_0^L \beta^2(x,t)e^{\mu x}\,\mathrm{d}x, \qquad (64)\\
\dot{V}_3 &= p_3\dot{\eta}(t)\int_0^L \frac{e^{\frac{\mu x}{2}}}{\lambda_2(x)}\beta(x,t)\,\mathrm{d}x + p_3\eta(t)\int_0^L \frac{e^{\frac{\mu x}{2}}}{\lambda_2(x)}\beta_t(x,t)\,\mathrm{d}x \\
&= p_3\left(\beta(0,t) - \alpha(0,t) + k_i^{-1}q_2\dot{\tilde{p}}(t)\right)\int_0^L \frac{e^{\frac{\mu x}{2}}}{\lambda_2(x)}\beta(x,t)\,\mathrm{d}x + p_3\eta(t)\beta(x,t)e^{\frac{\mu x}{2}}\Big|_0^L - \frac{\mu}{2}p_3\eta(t)\int_0^L \beta(x,t)e^{\frac{\mu x}{2}}\,\mathrm{d}x \\
&\leq \frac{q_4 L}{2}|p_3|\left((1-q_1)\beta(0,t) - k_i\eta(t) + k_i^{-1}q_2\dot{\tilde{p}}(t)\right)^2 + \frac{1}{2q_4}|p_3|\int_0^L \frac{e^{\mu x}}{\lambda_2^2(x)}\beta^2(x,t)\,\mathrm{d}x + p_3\frac{e^{\frac{\mu L}{2}}}{\kappa}\eta(t)\alpha(L,t) \\
&\quad - p_3\eta(t)\beta(0,t) - \frac{\mu}{2}p_3\eta(t)\int_0^L \beta(x,t)e^{\frac{\mu x}{2}}\,\mathrm{d}x, \\
&\leq \frac{3q_4 L}{2}|p_3|\left((1-q_1)^2\beta^2(0,t) + k_i^2\eta^2(t) + k_i^{-2}q_2^2\dot{\tilde{p}}^2(t)\right) + \frac{1}{2q_4}|p_3|\int_0^L \frac{e^{\mu x}}{\lambda_2^2(x)}\beta^2(x,t)\,\mathrm{d}x + p_3\frac{e^{\frac{\mu L}{2}}}{\kappa}\eta(t)\alpha(L,t) \\
&\quad - p_3\eta(t)\beta(0,t) - \frac{\mu}{2}p_3\eta(t)\int_0^L \beta(x,t)e^{\frac{\mu x}{2}}\,\mathrm{d}x, \qquad (65)\\
\dot{V}_4 &= (1-q_1)p_4 L\eta(t)\beta(0,t) - k_i p_4 L\eta^2(t) + k_i^{-1}q_2 p_4 L\eta(t)\dot{\tilde{p}}(t) \\
&\leq (1-q_1)p_4 L\eta(t)\beta(0,t) - k_i p_4 L\eta^2(t) + \frac{q_3}{2}|k_i^{-1}|q_2 p_4 L\eta^2(t) + \frac{1}{2q_3}|k_i^{-1}|q_2 p_4 L\dot{\tilde{p}}^2(t). \qquad (66)
\end{aligned}$$

Using (63)-(66), for all $t \geq 0$,

$$\dot{V} \leq -\theta V - \begin{bmatrix}\alpha(L,\cdot)\\ \beta(0,\cdot)\\ \eta(\cdot)\end{bmatrix}^{\top} M_1 \begin{bmatrix}\alpha(L,\cdot)\\ \beta(0,\cdot)\\ \eta(\cdot)\end{bmatrix} - \int_0^L \begin{bmatrix}\alpha(x,\cdot)\\ \beta(x,\cdot)\\ \eta(\cdot)\end{bmatrix}^{\top} M(x) \begin{bmatrix}\alpha(x,\cdot)\\ \beta(x,\cdot)\\ \eta(\cdot)\end{bmatrix}\mathrm{d}x + \left(\frac{3q_4 L}{2}|p_3|k_i^{-2}q_2^2 + \frac{1}{2q_3}|k_i^{-1}|q_2 p_4 L\right)\dot{\tilde{p}}^2(\cdot), \qquad (67)$$

where M_1 is given by (40) and

$$M(x) = \begin{bmatrix} A(x) & B^{\top}(x) \\ B(x) & C \end{bmatrix}, \qquad (68)$$

with

$$A(x) = \begin{bmatrix} \left(\mu p_1 - \frac{\theta p_1}{\lambda_1(x)}\right) e^{-\mu x} & 0 \\ 0 & \left(\mu p_2 - \frac{|p_3|}{2q_4\lambda_2^2(x)} - \frac{\theta p_2}{\lambda_2(x)}\right) e^{\mu x} \end{bmatrix}, \tag{69}$$

$$B(x) = \begin{bmatrix} 0 & \left(\frac{\mu p_3}{4} - \frac{\theta p_3}{2\lambda_2(x)}\right) e^{\frac{\mu x}{2}} \end{bmatrix}, \tag{70}$$

$$C = m(p_4 k_i - \frac{q_3}{2}|k_i^{-1}|q_2 p_4) - \frac{\theta p_4}{2}. \tag{71}$$

Therefore, using the Schur complement of C in $M(x)$ and (48), (71), for all x in $[0, L]$, $M(x) > 0$ holds if and only if

$$A(x) - B^\top(x)C^{-1}B(x) = \begin{bmatrix} M^{11}(x) & M^{12}(x) \\ * & M^{22}(x) \end{bmatrix} > 0 \tag{72}$$

with

$$M^{11}(x) = \left(\mu - \frac{\theta}{\lambda_1(x)}\right) p_1 e^{-\mu x}, \tag{73}$$

$$M^{12}(x) = 0, \tag{74}$$

$$M^{22}(x) = \left(\mu p_2 - \frac{|p_3|}{2q_4\lambda_2^2(x)} - \frac{\theta p_2}{\lambda_2(x)}\right) e^{\mu x} - \left(m(p_4 k_i - \frac{q_3}{2}|k_i^{-1}|q_2 p_4) - \frac{\theta p_4}{2}\right)^{-1} \left(\frac{\mu p_3}{4} - \frac{\theta p_3}{2\lambda_2(x)}\right)^2 e^{\mu x}. \tag{75}$$

Inequality (72) holds if and only if the conditions (48)-(50) are satisfied. Thus using (40), if $M(x) > 0$ holds,

$$\dot{V} \leq -\theta V + a_1 \dot{\tilde{p}}^2(\cdot), \tag{76}$$

with $a_1 = \frac{3q_4 L}{2}|p_3|k_i^{-2}q_2^2 + \frac{1}{2q_3}|k_i^{-1}|q_2 p_4 L > 0$, and thus along the solutions to the system (35)-(39),

$$V \leq e^{-\theta t}V(z_0) + a_1 e^{-\theta t}\int_0^t \dot{\tilde{p}}^2(s)e^{\theta s}\,\mathrm{d}s \leq e^{-\theta t}V(z_0) + a_1\int_0^t \dot{\tilde{p}}^2(s)\,\mathrm{d}s. \tag{77}$$

Combining this relation with (59), there exists positive constants $\Omega_1 \geq \frac{\lambda_{\max}}{\lambda_{min}}$, $b_1 \geq \frac{a_1}{\lambda_{\min}}$ such that

$$\begin{aligned} &\int_0^L \left(\alpha^2(x,t) + \beta^2(x,t)\right)\mathrm{d}x + L\eta^2(t) \\ &\leq \frac{1}{\lambda_{\min}} V \\ &\leq \frac{1}{\lambda_{\min}}\left(e^{-\theta t}V(z_0) + a_1\int_0^t \dot{\tilde{p}}^2(s)\,\mathrm{d}s\right) \\ &\leq \frac{1}{\lambda_{\min}}\left(e^{-\theta t}\cdot\lambda_{\max}\cdot\left(\int_0^L \left(\alpha^2(x,0) + \beta^2(x,0)\right)\mathrm{d}x + L\eta^2(0)\right) + a_1\int_0^t \dot{\tilde{p}}^2(s)\,\mathrm{d}s\right) \\ &\leq \Omega_1 e^{-\theta t}\left(\int_0^L \left(\alpha^2(x,0) + \beta^2(x,0)\right)\mathrm{d}x + L\eta^2(0)\right) + b_1\int_0^t \dot{\tilde{p}}^2(s)\,\mathrm{d}s, \end{aligned} \tag{78}$$

completing the proof of Theorem 1.

3.2 | Backstepping transformation and control law

In this section, a backstepping transformation is introduced to map the original system (26)-(34) into the target system (35)-(39). Consequently, we obtain the kernels in the introduced transformation by the kernel equations and the control law stabilizing the original system (26)-(34) by the mathematical expression involving these kernels.

As in [18], consider the backstepping transformation

$$\alpha(x,t) = \epsilon_1(x,t) - \int_x^L G^{11}(x,\xi)\epsilon_1(\xi,t)\,\mathrm{d}\xi - \int_x^L G^{12}(x,\xi)\epsilon_2(\xi,t)\,\mathrm{d}\xi, \tag{79}$$

$$\beta(x,t) = \epsilon_2(x,t) - \int_x^L G^{21}(x,\xi)\epsilon_1(\xi,t)\,\mathrm{d}\xi - \int_x^L G^{22}(x,\xi)\epsilon_2(\xi,t)\,\mathrm{d}\xi, \tag{80}$$

where $G^{11}(x,\xi)$, $G^{12}(x,\xi)$, $G^{21}(x,\xi)$ and $G^{22}(x,\xi)$ in $L^2((0,L)^2;\mathbb{R})$ are kernels in the triangular domain $\mathbb{T}_1 = \{(x,\xi) \in \mathbb{R}^2 \,|\, 0 \le x \le \xi \le L\}$.

Take time derivative and spatial derivative on the backstepping transformation (79) and (80), and substitute them into the target system (35)-(39) to get the following equations and boundary conditions of the kernels $G^{11}(x,\xi)$, $G^{12}(x,\xi)$, $G^{21}(x,\xi)$ and $G^{22}(x,\xi)$ from the original system (26)-(30) in the triangular domain $\mathbb{T}_1$.

The kernels $G^{11}(x,\xi)$, $G^{12}(x,\xi)$, $G^{21}(x,\xi)$ and $G^{22}(x,\xi)$ should satisfy the following kernel equations,

$$\lambda_1(x)G_x^{11}(x,\xi) + \lambda_1(\xi)G_\xi^{11}(x,\xi) = -\lambda_1'(\xi)G^{11}(x,\xi) + c_2(\xi)G^{12}(x,\xi), \tag{81}$$

$$\lambda_1(x)G_x^{12}(x,\xi) - \lambda_2(\xi)G_\xi^{12}(x,\xi) = \lambda_2'(\xi)G^{12}(x,\xi) + c_1(\xi)G^{11}(x,\xi), \tag{82}$$

$$\lambda_2(x)G_x^{21}(x,\xi) - \lambda_1(\xi)G_\xi^{21}(x,\xi) = \lambda_1'(\xi)G^{21}(x,\xi) - c_2(\xi)G^{22}(x,\xi), \tag{83}$$

$$\lambda_2(x)G_x^{22}(x,\xi) + \lambda_2(\xi)G_\xi^{22}(x,\xi) = -\lambda_2'(\xi)G^{22}(x,\xi) - c_1(\xi)G^{21}(x,\xi), \tag{84}$$

and the boundary conditions

$$G^{11}(x,L) = \frac{\lambda_2(L)}{\kappa\lambda_1(L)}G^{12}(x,L), \tag{85}$$

$$G^{12}(x,x) = \frac{c_1(x)}{\lambda_1(x)+\lambda_2(x)}, \tag{86}$$

$$G^{21}(x,x) = -\frac{c_2(x)}{\lambda_1(x)+\lambda_2(x)}, \tag{87}$$

$$G^{22}(x,L) = \frac{\kappa\lambda_1(L)}{\lambda_2(L)}G^{21}(x,L). \tag{88}$$

The well-posedness of the kernel equations (81)-(88) and the boundedness of kernel variables follow from a coordinate change $(x,\xi) \mapsto (L-\xi, L-x)$ and an application of Theorem A.1 in [18] in the triangular domain $\mathbb{T}_2 = \{(L-\xi, L-x) \in \mathbb{R}^2 \,|\, 0 \le L-\xi \le L-x \le L\}$. Therefore, for system (26)-(34), the following control law can be deduced,

$$\begin{aligned} U(t) = {} & \frac{k_i}{q_2}\int_0^t (\epsilon_2(0,s) - \epsilon_1(0,s))\,\mathrm{d}s \\ & + \frac{k_i}{q_2}\int_0^t\int_0^L \left[\left(G^{11}(0,\xi) - G^{21}(0,\xi)\right)\epsilon_1(\xi,s) + \left(G^{12}(0,\xi) - G^{22}(0,\xi)\right)\epsilon_2(\xi,s)\right]\mathrm{d}\xi\,\mathrm{d}s \\ & + \frac{1}{q_2}\int_0^L \left[\left(G^{11}(0,\xi) - q_1G^{21}(0,\xi)\right)\epsilon_1(\xi,t) + \left(G^{12}(0,\xi) - q_1G^{22}(0,\xi)\right)\epsilon_2(\xi,t)\right]\mathrm{d}\xi. \end{aligned} \tag{89}$$

Under the assumptions in the Theorem 1, the target system (35)-(39) is integral input-to-state stable. Thus, using the invertibility of backstepping transformation, the original system (26)-(34) is iISS in the L^2-norm with the control law (89).

Obviously, from (89), the practical implementation of the feedback control law needs the knowledge of the full state $(\epsilon_1(x,t),\epsilon_2(x,t))^\top$ over the whole spatial domain $[0,L]$. From (15), the output under coordinate transformation is

$$y(t)=\epsilon_2(0,t). \tag{90}$$

In the next section, the knowledge of the full state $(\epsilon_1(x,t),\epsilon_2(x,t))^\top$ in the control law $U(t)$ can be provided by a boundary state observer that uses the output $y(t)$ in (90) with a boundary measurement of $v(0,t)$ only. The kernels $G^{11}(0,\xi)$, $G^{12}(0,\xi)$, $G^{21}(0,\xi)$ and $G^{22}(0,\xi)$ can be derived by solving the kernel equations (81)-(88). Through choosing an appropriate value of k_i, the iISS of original system (26)-(34) is guaranteed with the control law (89).

4 | OBSERVER DESIGN AND OUTPUT FEEDBACK CONTROLLER

From (15), we note that the output $y(t)$ can be obtained by the measurement of inlet speed $v(0,t)$ of the considered road segment. In order to estimate the state $(\epsilon_1,\epsilon_2)^\top$, a boundary observer is designed as in [24] by constructing the system with the output injection terms:

$$\hat{\epsilon}_{1t}(x,t)+\lambda_1(x)\hat{\epsilon}_{1x}(x,t)+c_1(x)\hat{\epsilon}_2(x,t)=r(x)\left(y(t)-\hat{\epsilon}_2(0,t)\right), \tag{91}$$

$$\hat{\epsilon}_{2t}(x,t)-\lambda_2(x)\hat{\epsilon}_{2x}(x,t)+c_2(x)\hat{\epsilon}_1(x,t)=s(x)\left(y(t)-\hat{\epsilon}_2(0,t)\right), \tag{92}$$

$$\hat{\epsilon}_1(0,t)=q_1\hat{\epsilon}_2(0,t)-L_i\int_0^t\left(y(\tau)-\hat{\epsilon}_2(0,\tau)\right)\mathrm{d}\tau+q_2U(t), \tag{93}$$

$$\hat{\epsilon}_2(L,t)=\frac{1}{\kappa}\hat{\epsilon}_1(L,t). \tag{94}$$

In the previous equations, $\hat{\epsilon}_1$ and $\hat{\epsilon}_2$ are the estimates of the state variables ϵ_1 and ϵ_2, the terms $r(x)$ and $s(x)$ are the output injection gains, and $L_i\in\mathbb{R}\setminus\{0\}$ is an integral tuning parameter. In order to reject perturbation to guarantee the convergence of the estimated state to the real state, an integral term is added to a boundary condition of the observer. We design the boundary conditions of the observer system such that the mathematical expression of injection gains $r(x)$ and $s(x)$ are as simple as possible.

The objective is to use the backstepping transformation to find $r(x)$ and $s(x)$ such that $(\hat{\epsilon}_1,\hat{\epsilon}_2)^\top$ converges to $(\epsilon_1,\epsilon_2)^\top$. The error system can be obtained by subtracting the estimate system (91)-(94) from the original system (26)-(34) and (32)-(30),

$$\widetilde{\epsilon}_{1t}(x,t)+\lambda_1(x)\widetilde{\epsilon}_{1x}(x,t)+c_1(x)\widetilde{\epsilon}_2(x,t)=-r(x)\widetilde{\epsilon}_2(0,t), \tag{95}$$

$$\widetilde{\epsilon}_{2t}(x,t)-\lambda_2(x)\widetilde{\epsilon}_{2x}(x,t)+c_2(x)\widetilde{\epsilon}_1(x,t)=-s(x)\widetilde{\epsilon}_2(0,t), \tag{96}$$

$$\widetilde{\epsilon}_1(0,t)=q_1\widetilde{\epsilon}_2(0,t)+L_i\int_0^t\widetilde{\epsilon}_2(0,\tau)\,\mathrm{d}\tau+q_2\bar{p}(t), \tag{97}$$

$$\widetilde{\epsilon}_2(L,t)=\frac{1}{\kappa}\widetilde{\epsilon}_1(L,t), \tag{98}$$

where $\widetilde{\epsilon}_1(x,t)=\epsilon_1(x,t)-\hat{\epsilon}_1(x,t)$, and $\widetilde{\epsilon}_2(x,t)=\epsilon_2(x,t)-\hat{\epsilon}_2(x,t)$.

In order to guarantee the iISS of the error system (95)-(98), the target system (35)-(39) is mapped into the error system by using the backstepping transformation

$$\widetilde{\epsilon}_1(x,t) = \alpha(x,t) + \int_0^x F^{11}(x,\xi)\alpha(\xi,t)\,\mathrm{d}\xi + \int_0^x F^{12}(x,\xi)\beta(\xi,t)\,\mathrm{d}\xi, \tag{99}$$

$$\widetilde{\epsilon}_2(x,t) = \beta(x,t) + \int_0^x F^{21}(x,\xi)\alpha(\xi,t)\,\mathrm{d}\xi + \int_0^x F^{22}(x,\xi)\beta(\xi,t)\,\mathrm{d}\xi, \tag{100}$$

where the functions $F^{ij}(x,\xi)$ in $L^2((0,L)^2;\mathbb{R})$, $i,j = 1,2$ have to be determined in the triangular domain $\mathbb{T} = \{(x,\xi) \in \mathbb{R}^2 \,|\, 0 \le \xi \le x \le L\}$.

Differentiating the transformation (99) and (100) with respect to t and x, substituting the results into the error system (95)-(98) and using the equations of the target system (35)-(39), the following kernel equations and boundary conditions of the kernels $F^{11}(x,\xi)$, $F^{12}(x,\xi)$, $F^{21}(x,\xi)$ and $F^{22}(x,\xi)$ can be derived in the triangular domain $\mathbb{T}$,

$$\lambda_1(x)F_x^{11}(x,\xi) + \lambda_1(\xi)F_\xi^{11}(x,\xi) = -\lambda_1'(\xi)F^{11}(x,\xi) - c_1(x)F^{21}(x,\xi), \tag{101}$$

$$\lambda_1(x)F_x^{12}(x,\xi) - \lambda_2(\xi)F_\xi^{12}(x,\xi) = \lambda_2'(\xi)F^{12}(x,\xi) - c_1(x)F^{22}(x,\xi), \tag{102}$$

$$\lambda_2(x)F_x^{21}(x,\xi) - \lambda_1(\xi)F_\xi^{21}(x,\xi) = \lambda_1'(\xi)F^{21}(x,\xi) + c_2(x)F^{11}(x,\xi), \tag{103}$$

$$\lambda_2(x)F_x^{22}(x,\xi) + \lambda_2(\xi)F_\xi^{22}(x,\xi) = -\lambda_2'(\xi)F^{22}(x,\xi) + c_2(x)F^{12}(x,\xi), \tag{104}$$

with the boundary conditions

$$F^{11}(L,\xi) = \kappa F^{21}(L,\xi), \tag{105}$$

$$F^{12}(x,x) = -\frac{c_1(x)}{\lambda_1(x)+\lambda_2(x)}, \tag{106}$$

$$F^{21}(x,x) = \frac{c_2(x)}{\lambda_1(x)+\lambda_2(x)}, \tag{107}$$

$$F^{22}(L,\xi) = \frac{1}{\kappa}F^{12}(L,\xi). \tag{108}$$

The injection gains are, for all x in $[0,L]$,

$$r(x) = \lambda_2(0)F^{12}(x,0) - \left(1 - \frac{L_i}{k_i}\right)\lambda_1(0)F^{11}(x,0), \tag{109}$$

$$s(x) = \lambda_2(0)F^{22}(x,0) - \left(1 - \frac{L_i}{k_i}\right)\lambda_1(0)F^{21}(x,0). \tag{110}$$

The kernels $F^{11}(x,\xi)$, $F^{12}(x,\xi)$, $F^{21}(x,\xi)$ and $F^{22}(x,\xi)$ are the solutions to the kernel equations (101)-(108). The well-posedness of the solutions to kernel equations (101)-(108) is guaranteed by the Theorem A.1 in [18] in the triangular domain $\mathbb{T}_2$ following a coordinate change $(x,\xi) \mapsto (L-\xi, L-x)$.

Based on the reversibility of the backstepping transformation, it is straightforward to prove the iISS of the error system (95)-(98) in the L^2 sense through studying the stability of the target system (35)-(39). Let

$$\widetilde{\eta}(t) = \int_0^t \widetilde{\epsilon}_2(0,\tau)\,\mathrm{d}\tau + L_i^{-1}q_2\bar{p}(t). \tag{111}$$

Theorem 2 (iISS of Error System) *Under the assumptions of Theorem 1, consider the system (95)-(98), and the functions r*

and s respectively determined by (109) and (110), where $F^{11}(x,0)$, $F^{12}(x,0)$, $F^{21}(x,0)$ and $F^{22}(x,0)$ ($x \in [0, L]$) are obtained from (101)-(108), the equilibrium $\widetilde{\epsilon}_1 \equiv \widetilde{\epsilon}_2 \equiv 0$ is iISS in the L^2 sense, that is there exists positive constants Ω_2, b_2 such that, for any $(\widetilde{\epsilon}_1(\cdot,0), \widetilde{\epsilon}_2(\cdot,0))^\top$ in $L^2((0,L);\mathbb{R}^2)$, and for any $\bar{p}$ such that $\dot{\bar{p}} \in \mathcal{L}^2[0,\infty)$, the solution $(\widetilde{\epsilon}_1, \widetilde{\epsilon}_2, \widetilde{\eta})^\top$ to the system (95)-(98) and (111) satisfies

$$\int_0^L \left(\widetilde{\epsilon}_1^2(x,t) + \widetilde{\epsilon}_2^2(x,t)\right) \mathrm{d}x + L\widetilde{\eta}^2(t) \le \Omega_2 e^{-\theta t}\left(\int_0^L \left(\widetilde{\epsilon}_1^2(x,0) + \widetilde{\epsilon}_2^2(x,0)\right) \mathrm{d}x + L\widetilde{\eta}^2(0)\right) + b_2 \int_0^t \dot{\bar{p}}^2(s)\,\mathrm{d}s, \tag{112}$$

for all $t \ge 0$.

Since the transformation (99)-(100) is invertible, the dynamical behavior of (95)-(98) is the same as the behavior of the target system (35)-(39). Under the assumptions of Theorem 1, the target system (35)-(39) is integral input-to-state stable in the L^2 sense. Thus the iISS of (95)-(98) is obtained from the invertibility and linearity of the backstepping transformation, in other words, (112) holds.

Inspired by [32], a system is iISS implies that there is some output that makes the system weakly zero-detectable [34]. Moreover, on the basis of Theorem 2, as time t goes on, without disturbance $\bar{p}$, the state components $\hat{\epsilon}_1(x,t)$ and $\hat{\epsilon}_2(x,t)$ of the solutions to the observer (91)-(94) go to the real values $\epsilon_1(x,t)$ and $\epsilon_2(x,t)$. Therefore, the following observer-based output feedback controller is proposed by combining the full state feedback law (89) with the observer estimates (91)-(94),

$$\begin{aligned} U(t) = {} & \frac{k_i}{q_2}\int_0^t (y(s) - \hat{\epsilon}_1(0,s))\,\mathrm{d}s \\ & + \frac{k_i}{q_2}\int_0^t \int_0^L \left[\left(G^{11}(0,\xi) - G^{21}(0,\xi)\right)\hat{\epsilon}_1(\xi,s) + \left(G^{12}(0,\xi) - G^{22}(0,\xi)\right)\hat{\epsilon}_2(\xi,s)\right]\mathrm{d}\xi\,\mathrm{d}s \\ & + \frac{1}{q_2}\int_0^L \left[\left(G^{11}(0,\xi) - q_1 G^{21}(0,\xi)\right)\hat{\epsilon}_1(\xi,t) + \left(G^{12}(0,\xi) - q_1 G^{22}(0,\xi)\right)\hat{\epsilon}_2(\xi,t)\right]\mathrm{d}\xi, \end{aligned} \tag{113}$$

where $\hat{\epsilon}_1$ and $\hat{\epsilon}_2$ are computed from (91)-(94), the kernels $G^{11}(0,\xi)$, $G^{12}(0,\xi)$, $G^{21}(0,\xi)$ and $G^{22}(0,\xi)$ are computed from the kernel equations (81)-(88).

Combining Theorem 1 and Theorem 2, the following result can be derived, when closing the loop with the output feedback controller (113). The separation principle is used to proof the iISS of this closed-loop system and it was not applied to the infinite-dimensional systems before.

Theorem 3 (iISS of Closed-loop System) *Under the assumptions of Theorem 1, for any $(\epsilon_1(\cdot,0), \epsilon_2(\cdot,0), \widetilde{\epsilon}_1(\cdot,0), \widetilde{\epsilon}_2(\cdot,0))^\top$ in $L^2((0,L);\mathbb{R}^4)$ in $\mathbb{R}$, the observer-based output feedback controller (113) makes the equilibrium of the system (26)-(34) and (32)-(30) and the error system (95)-(98) iISS in the L^2 sense, that is there exists positive constants Ω_3, b_3 such that along the solution to (26)-(34), for any $\bar{p}$ such that $\dot{\bar{p}} \in \mathcal{L}^2[0,\infty)$, it holds, for all t in $[0,\infty)$,*

$$\begin{aligned} & \int_0^L \left(\epsilon_1^2(x,t) + \epsilon_2^2(x,t)\right)\mathrm{d}x + L\eta^2(t) + \int_0^L \left(\widetilde{\epsilon}_1^2(x,t) + \widetilde{\epsilon}_2^2(x,t)\right)\mathrm{d}x + L\widetilde{\eta}^2(t) \\ & \le \Omega_3 e^{-\theta t}\Big[\int_0^L \left(\epsilon_1^2(x,0) + \epsilon_2^2(x,0)\right)\mathrm{d}x + L\eta^2(0) + \int_0^L \left(\widetilde{\epsilon}_1^2(x,0) + \widetilde{\epsilon}_2^2(x,0)\right)\mathrm{d}x + L\widetilde{\eta}^2(0)\Big] + b_3\int_0^t \dot{\bar{p}}^2(s)\,\mathrm{d}s. \end{aligned} \tag{114}$$

Proof The following candidate Lyapunov function is proposed,

$$W = W_1 + W_2, \tag{115}$$

where

$$W_1 = \int_0^L \begin{bmatrix} \epsilon_1(x,t) \\ \epsilon_2(x,t) \\ \eta(t) \end{bmatrix}^\top P_1(x) \begin{bmatrix} \epsilon_1(x,t) \\ \epsilon_2(x,t) \\ \eta(t) \end{bmatrix} \mathrm{d}x, \tag{116}$$

$$W_2 = \int_0^L \begin{bmatrix} \widetilde{\epsilon}_1(x,t) \\ \widetilde{\epsilon}_2(x,t) \\ \widetilde{\eta}(t) \end{bmatrix}^\top P_2(x) \begin{bmatrix} \widetilde{\epsilon}_1(x,t) \\ \widetilde{\epsilon}_2(x,t) \\ \widetilde{\eta}(t) \end{bmatrix} \mathrm{d}x, \tag{117}$$

with

$$P_j(x) = \begin{bmatrix} \frac{p_{j1}}{\lambda_1(x)} e^{-\mu x} & 0 & 0 \\ * & \frac{p_{j2}}{\lambda_2(x)} e^{\mu x} & \frac{p_{j3}}{2\lambda_2(x)} e^{\frac{\mu x}{2}} \\ * & * & \frac{p_{j4}}{2} \end{bmatrix}, \quad j = 1, 2, \quad \text{for all } x \in (0, L). \tag{118}$$

From Theorem 1 and the invertibility and linearity of the backstepping transformation, for the system (26)-(34) and (32)-(30), there exist positive constants $p_{11}, p_{12}, p_{14}, C, a_1, b$ and a constant p_{13} such that

$$\dot{W}_1 \leq -\theta W_1 + a_1 \dot{\hat{p}}^2, \tag{119}$$

and

$$\int_0^L \left(\epsilon_1^2(x,t) + \epsilon_2^2(x,t)\right) \mathrm{d}x + L\eta^2(t) \leq Ce^{-\theta t} \left(\int_0^L \left(\epsilon_1^2(x,0) + \epsilon_2^2(x,0)\right) \mathrm{d}x + L\eta^2(0) \right) + b \int_0^t \dot{\hat{p}}^2(s)\, \mathrm{d}s. \tag{120}$$

From Theorem 2, the iISS of the error system (95)-(98) guarantees exact estimation of the state ϵ_1 and ϵ_2 of the system (26)-(30) under the assumptions of Theorem 1, i.e., there exist positive constants $p_{21}, p_{22}, p_{24}, a_2$ and a constant p_{23} such that

$$\dot{W}_2 \leq -\theta W_2 + a_2 \dot{\tilde{p}}^2. \tag{121}$$

and (112) hold.

According to the separation principle, and the inequalities (119)-(121), the Lyapunov function W for the output feedback closed-loop system consisting of the original system (26)-(34) and (32)-(30) and the error system (95)-(98) satisfies

$$\dot{W} = \dot{W}_1 + \dot{W}_2 \leq -\theta W + (a_1 + a_2)\dot{\tilde{p}}^2, \tag{122}$$

Then for $\Omega_3 \geq \max\{\Omega_2, C\}$, $b_3 = b + b_2$, one can derive the following result from (112) and (120),

$$\begin{aligned} &\int_0^L \left(\epsilon_1^2(x,t) + \epsilon_2^2(x,t)\right) \mathrm{d}x + L\eta^2(t) + \int_0^L \left(\widetilde{\epsilon}_1^2(x,t) + \widetilde{\epsilon}_2^2(x,t)\right) \mathrm{d}x + L\widetilde{\eta}^2(t) \\ &\leq \Omega_3 e^{-\theta t} \Big[\int_0^L \left(\epsilon_1^2(x,0) + \epsilon_2^2(x,0)\right) \mathrm{d}x + L\eta^2(0) + \int_0^L \left(\widetilde{\epsilon}_1^2(x,0) + \widetilde{\epsilon}_2^2(x,0)\right) \mathrm{d}x + L\widetilde{\eta}^2(0) \Big] + b_3 \int_0^t \dot{\tilde{p}}^2(s)\, \mathrm{d}s. \end{aligned} \tag{123}$$

Therefore, it is proved that with the control law (113), the equilibrium $\epsilon_1 \equiv \epsilon_2 \equiv 0$ of the system (26)-(34) and (32)-(30) is iISS in the L^2 sense.

5 | OPTIMAL CONTROLLER AND NUMERICAL STUDIES

5.1 | Optimal controller

In order to seek the optimal control law $U(t)$ in (113), the following optimization problem for the maximal θ can be considered to derive the optimal value of k_i:

$$\begin{aligned} &\max\ \theta \\ &\text{subject to } \mu, \theta, p_1, p_2, p_4, q_3, q_4 > 0, \text{and (40)-(50) for all } x \in [0, L]. \end{aligned} \tag{124}$$

Checking the constraints above, ask to deal with the matrix inequalities that are not directly numerically tackled due to the products between unknown parameters. The parameters k_i, μ, θ, m can be given through line search methods, and the other variables p_1, p_2, p_3, p_4 can be derived by solving linear matrix inequalities (LMIs). We discretize the spatial variable x on the domain $[0, L]$ to solve infinite LMIs.

Remark The parameters k_i, μ and θ have effects on the iISS of the target system in terms of the matrix inequalities. The parameter k_i serves as the integral tuning parameter at the boundary $x = 0$ of the target system, and it is the key parameter to determine the iISS property in the L^2 sense. The positive constant μ is involved in the exponent or power of the exponential terms of the Lyapunov function that is proposed to analyze the stability of the target system. It has also an effect on the condition number of the matrix M_1 in (40). The parameter θ is the exponential rate of convergence of the target system, the error system and the closed-loop system. The higher θ is, the faster the closed-loop system converges. Selecting the fitting parameters k_i, μ and θ is done by three independent line searches and three different loops.

5.2 | Simulations

In order to demonstrate the performance of the proposed controller (113) in stabilizing the system (26)-(30) around the equilibrium, numerical simulations are done in this section. Given $\bar{\rho}(t), \omega^*(x), v^*(x)$, compute controller for the linearized system and simulate the nonlinear model. For simulations, we illustrate by rush hour the traffic demand $\bar{\rho}(t)$ serving as an exogenous variable for traffic flow model that varies on time scales.

For numerical simulations, the traffic parameters of a local road section under consideration are chosen as in [13]: $L = 1\,\text{km}$, $v_f = 150\,\text{km/h}$, $\rho_m = 200\,\text{veh./km}$, $\tau = 60\,\text{s}$, $\bar{\rho}(t) = 420e^{-10t}\,(\text{veh./h})$, $t \in [0, \infty)$. The steady state is chosen as $\rho^*(x) = 120 - 0.5x\,(\text{veh./km})$, $v^*(x) = 70 - 0.5x\,(\text{km/h})$, $x \in [0, L]$ which leads to the characteristic speeds $\lambda_1 = 70 - 0.5x$, and $\lambda_2 = 20 + 0.125x$, $x \in [0, L]$, then $q_1 = -0.2857$, $q_2 = 0.0107$, $q_3 = 1$, $q_4 = 1$, $\kappa = 2.2487$. The initial conditions are defined as

$$\begin{aligned} \rho(x, 0) &= \rho^*(x) + 0.5 \sin 4\pi x, \\ v(x, 0) &= v^*(x) + 1.8 \cos 4\pi x. \end{aligned}$$

Solving (124) by using Matlab, Figure 2 shows the relation between maximal θ and parameter k_i. It is checked in this

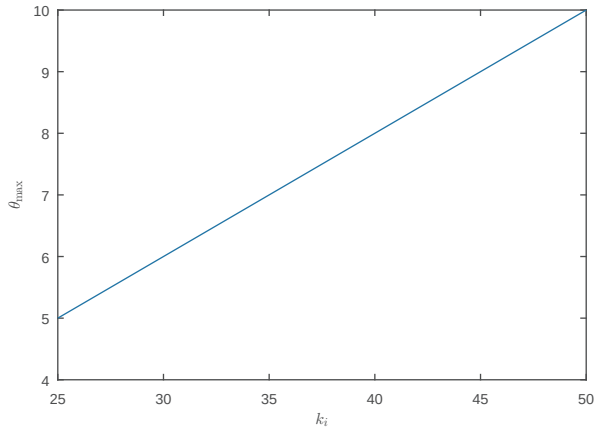

FIGURE 2 Relation between $\theta_{\max}$ and k_i.

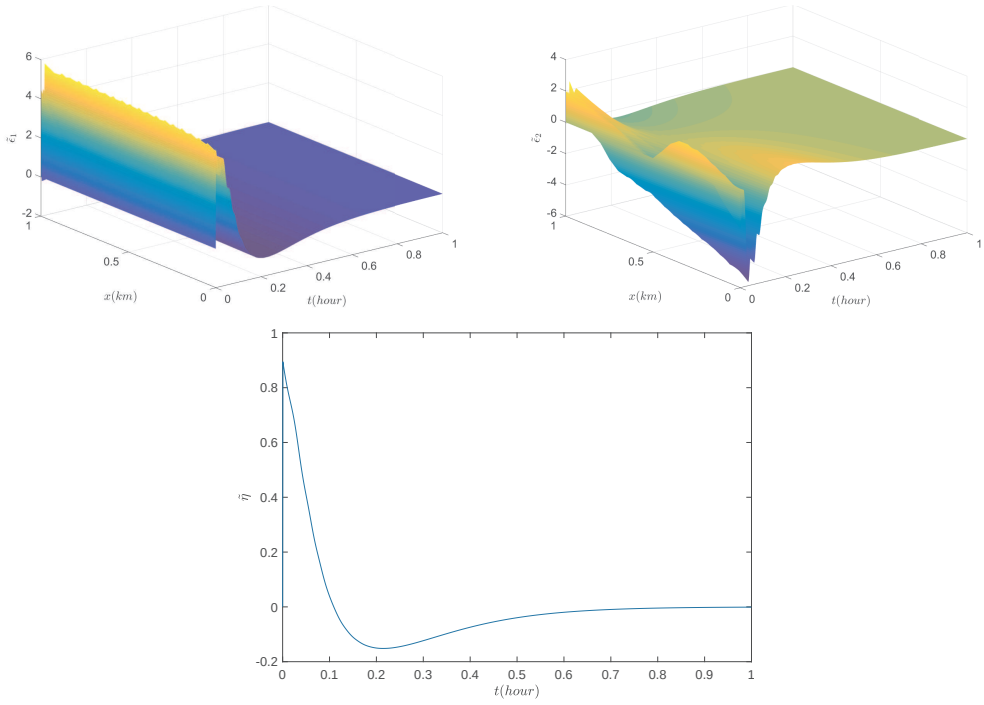

FIGURE 3 State $(\widetilde{e}_1, \widetilde{e}_2, \widetilde{\eta})^\top$ of the error system.

figure that the larger k_i is, the larger is $\theta_{\max}$ given by (124). This figure can be used to compute the best performance, given an amplitude constraint on k_i. Choosing the control gain $k_i = 35$ in (89) and (113), $\mu = 0.6$, and $m = 0.1$, we get $\theta = 7, p_1 = 10.6524, p_2 = 15.966, p_3 = 0.0059, p_4 = 564.0186$, so that (40)-(50) hold. The integral tuning parameter is set $L_i = 5$ in (98), and using the method described and the code attached in Appendix F.2 of [27], the values of

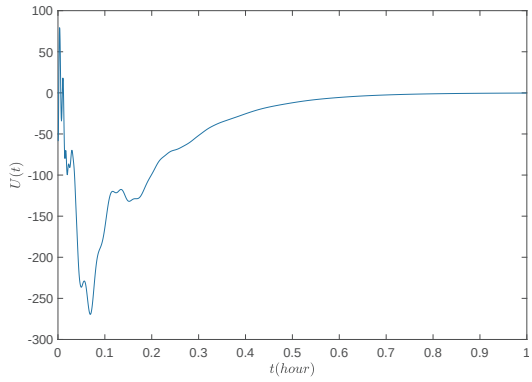

FIGURE 4 Evolution of the observer-based output feedback controller $U(t)$.

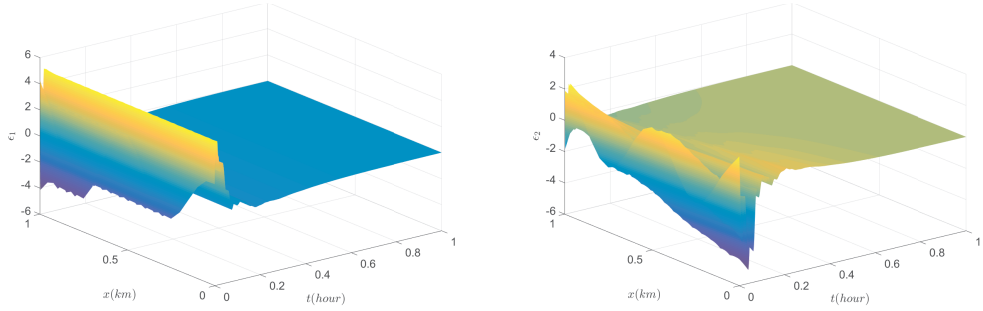

FIGURE 5 State $(\epsilon_1, \epsilon_2)^\top$ of the original system in closed loop with the optimal observer-based output feedback controller.

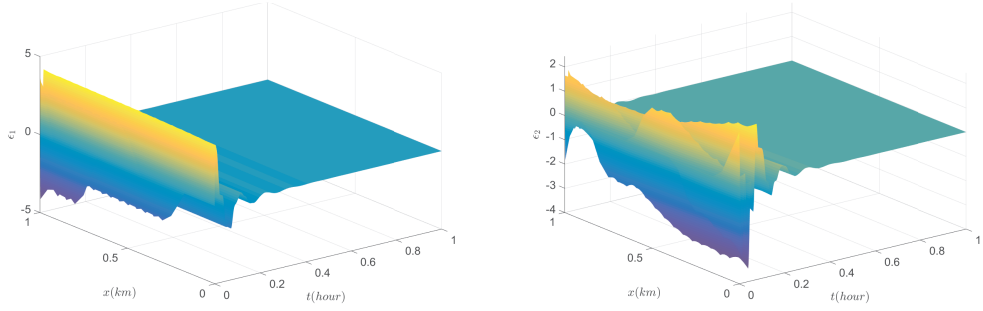

FIGURE 6 State $(\epsilon_1, \epsilon_2)^\top$ of the original system with the full state feedback controller.

kernels $G^{11}, G^{12}, G^{21}, G^{22}$ at $x = 0$ are derived from numerical computation of the kernel equations (81)-(88) and the values of $F^{11}, F^{12}, F^{21}, F^{22}$ at $x = 0$ are obtained from the numerical computation of (101)-(108). Different from the

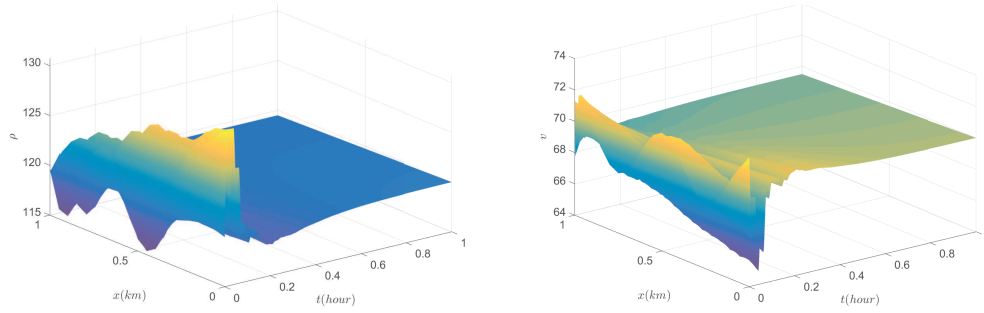

FIGURE 7 State $(\rho, v)^\top$ of the plant system in closed loop with the optimal observer-based output feedback controller.

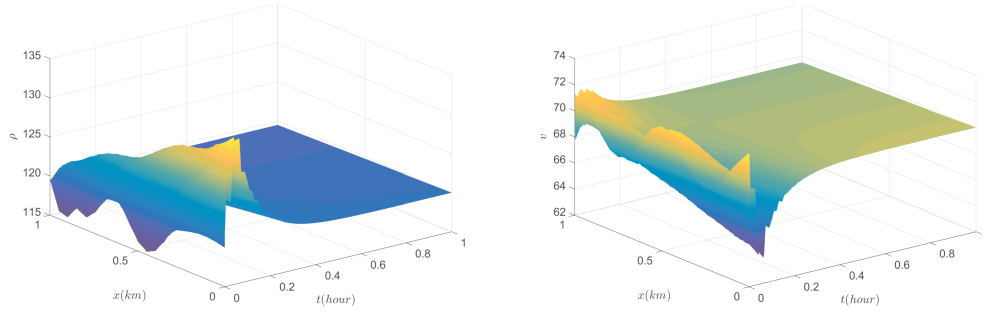

FIGURE 8 State $(\rho, v)^\top$ of the plant system in open loop.

previous research giving the explicit formula of backstepping transformations that can be used to deduce the explicit solutions of kernels, the numerical solutions of kernels in the general formation of backstepping transformations can be derived using [27].

The iISS of the error system can be seen in Figure 3. The evolution of the output feedback controller $U(t)$ given by (113) is given in Figure 4. In Figure 5, the state of the closed-loop system with the output feedback control converges to zero steady state. This numerical result is consistent with Theorem 3. By comparing Figure 5 and Figure 6, it is obvious that the observer maintains the exponential convergence performance of the closed-loop system, and it is also capable of estimating the full states of the system only by one boundary measurement as described earlier. Figure 7 gives the numerical simulations of the nonlinear ARZ traffic model in closed loop with the controller that is computed with the linearized model. It is obvious that the designed observer-based output feedback controller for the linearized ARZ traffic system stabilizes the nonlinear system in the same way. Moreover, comparing the convergence speeds in open loop (nearly 0.4 hours in Figure 8) and in closed loop with the optimal controller (nearly 0.2 hours in Figure 7), we check that the system converges to the steady state with the fastest speed using the designed optimal controller.

6 | CONCLUSION

The stabilization of the nonlinear Aw-Rascle-Zhang (ARZ) congestion traffic flow model with an unknown perturbation at the upstream boundary was considered in this paper. A full-state feedback controller was designed to stabilize the linear part of the nonlinear ARZ model. By designing an exponentially convergent observer which only needs to measure the upstream boundary state, an output state feedback controller and the iISS were achieved. Only the upstream inlet vehicles velocity was measured for the design of control law and the unpredicted perturbation was rejected by designing proper injection gains of the observer.

With the same method, some related problems could be considered. Instead of the congested regime, the free-flow regime will be studied in the future research work. Moreover, it could be a great help to apply our approach to some other models or other balance laws rather than the traffic flow model. The method also can be used for other hyperbolic systems with more than two eigenvalues. We may also investigate the observer-based output feedback control for nonlinear systems. We also may introduce some new technologies for the future research work, such as the event-triggered communication technique and the neural network technique.

7 | DATA AVAILABILITY STATEMENT

Data sharing is not applicable to this article as no new data were created or analyzed in this study.

references

[1] Treiber M, Kesting A. Traffic Flow Dynamics: Data, Models and Simulation. Springer; 2012.

[2] Lighthill MJ, Whitham GB. On kinematic waves II. A theory of traffic flow on long crowded roads. Proceedings of the Royal Society A: Mathematical, Physical and Engineering Sciences 1955;229(1178):317–345.

[3] Richards PI. Shock waves on the highway. Operations Research 1956;4(1):42–51.

[4] Payne HJ. Models of Freeway Traffic and Control. Mathematical Models of Public Systems 1971;1:51–61.

[5] Whitham GB. Linear and nonlinear waves. Pure and Applied Mathematics: A Wiley Series of Texts, Monographs and Tracts, Wiley-Interscience; 1999.

[6] Aw A, Rascle M. Resurrection of "second order" models of traffic flow. SIAM J Appl Math 2000;60(3):916–938.

[7] Zhang HM. A non-equilibrium traffic model devoid of gas-like behavior. Transportation Research Part B 2002;36(3):275–290.

[8] Cassidy MJ, Windover JR. Methodology for assessing dynamics of freeway traffic flow. Transportation Research Record 1995;1484:73–79.

[9] Daganzo CF. Requiem for second-order fluid approximations of traffic flow. Transportation Research Part B Methodological 1995;29(4):277–286.

[10] Mollier S, Delle Monache ML, Canudas-de-Wit C, Seibold B. Two-dimensional macroscopic model for large scale traffic networks. Transportation Research Part B: Methodological 2019;122:309–326.

[11] Belletti F, Huo M, Litrico X, Bayen AM. Prediction of traffic convective instability with spectral analysis of the Aw-Rascle-Zhang model. Physics Letters A 2015;379(38):2319–2330.

[12] Zhang L, Prieur C. Necessary and sufficient conditions on the exponential stability of positive hyperbolic systems. IEEE Transactions on Automatic Control 2017;62(7):3610–3617.

[13] Zhang L, Prieur C, Qiao J. PI boundary control of linear hyperbolic balance laws with stabilization of ARZ traffic flow models. Systems & Control Letters 2019;123:85–91.

[14] Blandin S, Litrico X, Delle Monache ML, Piccoli B, Bayen A. Regularity and Lyapunov stabilization of weak entropy solutions to scalar conservation laws. IEEE Transactions on Automatic Control 2016;62(4):1620–1635.

[15] Krstic M, Smyshlyaev A. Backstepping boundary control for first-order hyperbolic PDEs and application to systems with actuator and sensor delays. Systems and Control Letters 2008;57(9):750–758.

[16] Krstic M. Boundary control of PDEs: A course on backstepping design. Philadelphia, PA, USA: Society for Industrial and Applied Mathematics; 2008.

[17] Smyshlyaev A, Cerpa E, Krstic M. Boundary Stabilization of a 1-D Wave Equation with In-Domain Antidamping. SIAM J Control Optim 2010;48(6):4014–4031.

[18] Coron JM, Vazquez R, Krstic M, Bastin G. Local Exponential H^2 Stabilization of a 2×2 Quasilinear Hyperbolic System Using Backstepping. SIAM Journal on Control and Optimization 2013;51(3):2005–2035.

[19] Deutscher J. Backstepping Design of Robust State Feedback Regulators for Linear 2×2 Hyperbolic Systems. IEEE Transactions on Automatic Control 2017;62(10):5240–5247.

[20] Deutscher J. Finite-time output regulation for linear 2×2 hyperbolic systems using backstepping. Automatica 2017;75:54–62.

[21] Anfinsen H, Aamo OM. Adaptive control of linear 2×2 hyperbolic systems. Automatica 2018;87:69–82.

[22] Yu H, Gan Q, Bayen A, Krstic M. PDE Traffic Observer Validated on Freeway Data. IEEE Transactions on Control Systems Technology 2020;p. 1–13.

[23] Auriol J. Output feedback stabilization of an underactuated cascade network of interconnected linear PDE systems using a backstepping approach. Automatica 2020;117:108964. http://www.sciencedirect.com/science/article/pii/S000510982030162X.

[24] Vazquez R, Krstic M, Coron JM. Backstepping boundary stabilization and state estimation of a 2×2 linear hyperbolic system. Orlando, FL: IEEE Conference on Decision and Control and European Control Conference; 2011. p. 4937–4942.

[25] Yu H, Krstic M. Traffic congestion control for Aw-Rascle-Zhang model. Automatica 2019;100:38–51.

[26] Aamo OM. Disturbance rejection in 2 x 2 linear hyperbolic systems. IEEE Transactions on Automatic Control 2013;58(5):1095–1106.

[27] Anfinsen H, Aamo OM. Adaptive Control of Hyperbolic PDEs. Communications and Control Engineering, Springer; 2019.

[28] Yu H, Koga S, Oliveira TR, Krstic M. Extremum Seeking for Traffic Congestion Control With a Downstream Bottleneck. Journal of Dynamic Systems, Measurement, and Control 2020 10;143(3). https://doi.org/10.1115/1.4048781, 031007.

[29] Zeng J, Qian Y, Lv Z, Yin F, Zhu L, Zhang Y, et al. Expressway traffic flow under the combined bottleneck of accident and on-ramp in framework of Kerner's three-phase traffic theory. Physica A: Statistical Mechanics and its Applications 2021;574:125918. https://www.sciencedirect.com/science/article/pii/S0378437121001904.

[30] Martínez I, Jin WL. Optimal location problem for variable speed limit application areas. Transportation Research Part B: Methodological 2020;138:221–246. https://www.sciencedirect.com/science/article/pii/S0191261520303167.

[31] Greenshields B, Bibbins J, Channing W, Miller H. A study of traffic capacity. Highway research board proceedings 1935;14:448–477.

[32] Angeli D, Sontag ED, Wang Y. A characterization of integral input-to-state stability. IEEE Transactions on Automatic Control 2000;45(6):1082–1097.

[33] Mironchenko A, Ito H. Construction of Lyapunov Functions for Interconnected Parabolic Systems: An iISS Approach. SIAM Journal on Control and Optimization 2015;53(6):3364–3382. https://doi.org/10.1137/14097269X.

[34] Byrnes C, Isidori A, Willems J. Passivity, feedback equivalence, and the global stabilization of minimum phase nonlinear systems. IEEE Transactions on Automatic Control 1991;36:1228–1240.